

Direct observation of dynamic local structure in $\text{La}_{2-x}\text{Sr}_x\text{CuO}_4$ around $x=0.12$

Y. Horibe

Department of Materials Science and Engineering, Waseda University, Shinjuku-ku, Tokyo 169, Japan

Y. Inoue

Structural Analysis Section, Research Department, Nissan ARC Ltd., 1 Natsushima-cho, Yokosuka, Kanagawa 237, Japan

Y. Koyama

*Department of Materials Science and Engineering, Waseda University, Shinjuku-ku, Tokyo 169, Japan
and Kagami Memorial Laboratory for Materials Science and Technology, Advanced Research Center for Science and Engineering,
Waseda University, Shinjuku-ku, Tokyo 169, Japan*

(Received 30 August 1999)

In situ observation of the dynamic local structure in $\text{La}_{2-x}\text{Sr}_x\text{CuO}_4$ has been conducted at lower temperatures by transmission electron microscopy. The observation clearly showed that around $x=0.12$ dynamic fluctuation of the local *Pccn*/*LTT*-tilt region in the interior of the LTO domain occurs, even at 12 K, while *Pccn*/*LTT* regions nucleated along the twin boundary are rather static. The dynamic local *Pccn*/*LTT* region is thought to play a crucial role in the slight suppression of T_C and in the appearance of the incommensurate magnetic structure, both of which have been reported to occur around $x=0.12$.

I. INTRODUCTION

Among successive structural phase transitions occurring in La cuprates, structural changes from low-temperature orthorhombic (LTO) to *Pccn* and then to low-temperature tetragonal (LTT) are called low-temperature structural phase transitions.¹⁻⁸ In our previous work on the low-temperature transitions in Nd-substituted $\text{La}_{1.5}\text{Sr}_{0.1}\text{Nd}_{0.4}\text{CuO}_4$ by transmission electron microscopy, it was found that the transitions proceed together with the dynamic fluctuation of local *Pccn*/*LTT*-tilt regions.^{9,10} The dynamic fluctuation is a consequence of the competition between the tilt of the oxygen octahedron and the spontaneous strain e_4 , which are, respectively, the local and strain order parameters in the structural transition. In $\text{La}_{2-x}\text{Sr}_x\text{CuO}_4$ where the low-temperature transition has not been detected by x-ray and neutron powder diffractions, it can be expected that the dynamic local structure appears at lower temperatures as the equilibrium fluctuation of the local order parameter. In the present work, we examined the presence of such equilibrium fluctuation in $\text{La}_{2-x}\text{Sr}_x\text{CuO}_4$ by transmission electron microscopy.

The equilibrium fluctuation of the order parameter was suggested theoretically in relation to the origin of the tweed texture, which has been observed in a parent phase of the first-order ferroelastic transition.^{11,12} Parlinski *et al.* investigated features of the texture in the ferroelastic tetragonal to orthorhombic phase transition of $\text{YBa}_2\text{Cu}_3\text{O}_{7-\delta}$ by computer simulation.¹² It should be noted that the local and strain order parameters are, respectively, the occupation probability of the oxygen site and the strain from tetragonal to orthorhombic. One interesting feature they found is that at temperatures well above the transition temperature there are embryos of the tweed, which can be identified as the equilibrium fluctuation of the order parameter. It was also pointed out that the anisotropic long-range nature of the strain plays a crucial role in the equilibrium fluctuation. A similar situation occurs

in the low-temperature structural phase transitions in La cuprates. As was mentioned here, the equilibrium fluctuation of the local order parameter should occur in $\text{La}_{2-x}\text{Sr}_x\text{CuO}_4$.

We have already made a preliminary examination of the low-temperature structural phase transitions in $\text{La}_{2-x}\text{Sr}_x\text{CuO}_4$ with $x=0.115$ and 0.15 by transmission electron microscopy.^{13,14} It was reported that the *Pccn*/*LTT*-tilt region is nucleated along the LTO twin boundary at a transition temperature T_L in both oxides and that only in $x=0.115$ does the region also appear in the interior of the LTO domain. At that time, unfortunately, the dynamic nature of these local *Pccn*/*LTT*-tilt regions had not been confirmed. In the present work, we examined the existence and features of the dynamic fluctuation of the *Pccn*/*LTT*-tilt region in $\text{La}_{2-x}\text{Sr}_x\text{CuO}_4$ by transmission electron microscopy, along with confirming the low-temperature structural phase transitions. On the basis of the experimental data obtained in this study, we discuss not only the stability of the *Pccn*/*LTT*-tilt region, but also the relation between the dynamic *Pccn*/*LTT*-tilt region and other phenomena such as T_C suppression and the incommensurate magnetic structure. Both the slight suppression of T_C and the appearance of the incommensurate magnetic structure have been reported around $x=0.12$.¹⁵⁻²⁰

II. EXPERIMENTAL PROCEDURE

$\text{La}_{2-x}\text{Sr}_x\text{CuO}_4$ ceramic samples with $x=0.10$, 0.115, 0.12, and 0.15 were prepared for examination. The details of sample preparation are explained elsewhere.^{10,13} *In situ* observation of the dynamic local region as well as the low-temperature structural phase transitions was performed between room temperature and 12 K by using an H-800 transmission electron microscope with the help of a cooling stage equipped with a liquid He reservoir. A series of dark field images were taken at a time interval of about 6 sec by using 100-type forbidden spots in order to elucidate the dy-

dynamic nature of the *Pccn*/*LTT*-tilt region. Imaging plates were used as the recording medium to avoid sample drift. It should be mentioned here that in the diffraction patterns the *Pccn* and *LTT* tilts of the octahedron are both characterized by the 100-type forbidden spots for the *HTT* and *LTO* structures. Since this makes it impossible to distinguish between the *Pccn* and *LTT* structures experimentally, the expression *Pccn*/*LTT* structure (phase) will be used without distinction in this paper.

III. EXPERIMENTAL RESULTS

The low-temperature structural phase transition in $\text{La}_{2-x}\text{Sr}_x\text{CuO}_4$ was confirmed in all samples by the appearance of the *Pccn*/*LTT*-tilt region along the *LTO* twin boundary. Only the $x=0.115$ and 0.12 samples exhibited the dynamic fluctuation of the local *Pccn*/*LTT*-tilt region in the interior of the *LTO* domain. The experimental data presented here will be the results for the $x=0.10$ and 0.12 samples.

The $x=0.1$ sample, $\text{La}_{1.9}\text{Sr}_{0.1}\text{CuO}_4$, underwent a low-temperature structural transition around $T_L=165$ K, which was determined from the appearance of the 100-type forbidden spots in electron diffraction patterns. Figures 1(a), 1(b), and 1(c) are a bright-field image, a 100 forbidden dark-field image, and a corresponding electron diffraction pattern of the $x=0.1$ sample at 12 K, respectively. The electron incidence is parallel to the $[001]$ direction, and diffraction spots are indexed in terms of the *HTT* structure. The exposure time of the dark-field image was about 1.5 sec. In addition to fundamental spots due to the *LTO* structure, there are 100-type forbidden spots, indicating the appearance of the *Pccn*/*LTT*-tilt region, as denoted by arrow *A* in the diffraction pattern. Also observed are diffraction spots denoted as *B* at $1/2\ 1/2\ 0$ -type positions, whose origin was discussed in our previous paper.⁸ On the other hand, only a banded contrast is seen in the bright-field image. The contrast was found to be identical to that due to the twin structure in the *LTO* phase. That is, the *LTO* twin domain still exists at 12 K, well below T_L of about 165 K. We then took the dark-field image in Fig. 1(b) by using the 100 forbidden spot. The *Pccn*/*LTT*-tilt regions are clearly seen as a bright-line-contrast region. The width of the region was estimated to be about 10 nm. Note that the contrast in the image is diffraction contrast. From a comparison with the bright-field image in Fig. 1(a), the *Pccn*/*LTT* region was also found to appear along the *LTO* twin boundary between two neighboring *LTO* domains. A significant feature of the image is that no *Pccn*/*LTT*-tilt region exists in the interior of the *LTO* domain, even at the lowest temperature of 12 K. In other words, the low-temperature structural phase transition in the $x=0.1$ sample is characterized only by the appearance of the *Pccn*/*LTT*-tilt region along the *LTO* twin boundary. It should be mentioned that because the volume fraction of the *Pccn*/*LTT*-tilt region along the twin boundary was very low, as seen in Fig. 1(a), it was very hard to detect the low-temperature structural transition by means of x-ray and neutron powder diffractions.

Figures 2(a) and 2(b) are, respectively, a 100 forbidden dark-field image and a corresponding electron diffraction pattern of the $x=0.12$ sample at 85 K. The electron incidence is parallel to the $[001]$ direction, and diffraction spots

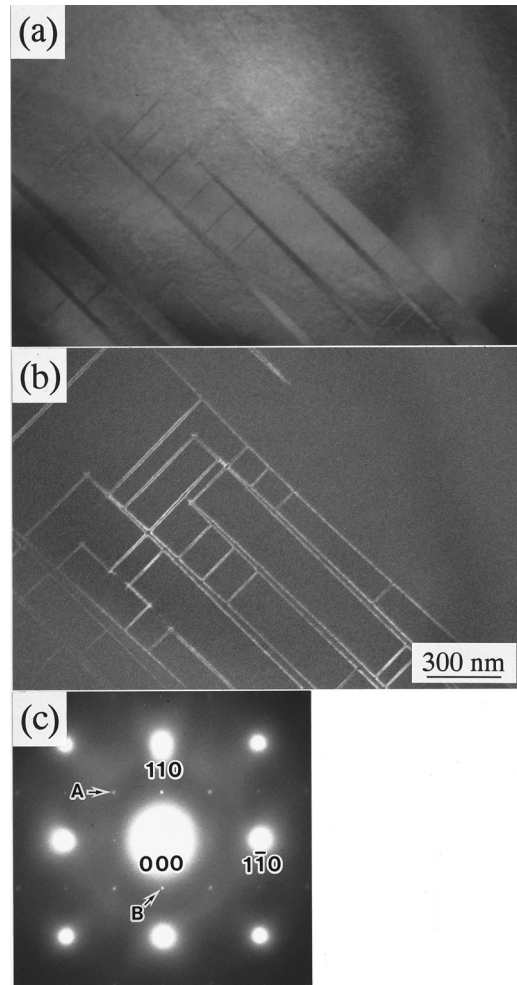


FIG. 1. (a) Bright-field image, (b) a 100 forbidden dark-field image, and (c) a corresponding electron diffraction pattern of the $x=0.1$ sample, $\text{La}_{1.90}\text{Sr}_{0.10}\text{CuO}_4$, at 12 K. The electron incidence is parallel to the $[001]$ direction, and diffraction spots are indexed in *HTT* notation.

are indexed in *HTT* notation. The transition temperature T_L , determined from the appearance of the 100-type forbidden spots, was about 135 K in the $x=0.12$ sample. In the pattern in Fig. 2(b), 100-type forbidden spots and the $1/2\ 1/2\ 0$ -type superlattice spots are seen, in addition to the fundamental spots due to the *LTO* structure. It is obvious that the 100-type spots are an indication of the *Pccn*/*LTT*-tilt region. In the 100 dark-field image, the *Pccn*/*LTT*-tilt regions are observed only as a bright-line-contrast region with an average width of about 10 nm, just as in the case of the $x=0.10$ sample at 12 K. Since there is no bright-contrast region in the interior of the *LTO* domain, the *Pccn*/*LTT*-tilt region is present only along the *LTO* twin boundary at 85 K.

The dynamic fluctuation of the *Pccn*/*LTT*-tilt region in the interior of the *LTO* domain was observed below about 40 K in the $x=0.12$ sample. Figure 3 shows a 100 forbidden dark-field image at 12 K, which was obtained by the subsequent cooling of the sample after the image in Fig. 2(a) was taken. The line-contrast regions are observed as bright contrast along the twin boundary. The average width of the region at 12 K was about 15 nm, which was slightly larger than that at 85 K. These results indicate that upon cooling lateral

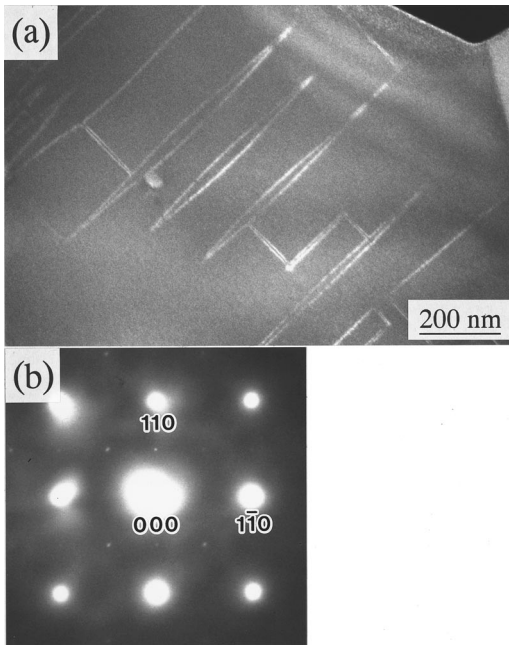


FIG. 2. (a) 100 forbidden dark-field image and (b) a corresponding electron diffraction pattern of the $x=0.12$ sample, $\text{La}_{1.88}\text{Sr}_{0.12}\text{CuO}_4$, at 85 K. The electron incidence is parallel to the $[001]$ direction.

growth of the *Pccn*/*LTT*-tilt region nucleated along the twin boundary is not conspicuous. The most striking feature of the image at 12 K is that *Pccn*/*LTT*-tilt regions are clearly seen as bright contrast in the interior of the LTO domain, as indicated by the arrow. These *Pccn*/*LTT*-tilt regions exhibit dynamic behavior, which depends upon the size of the region and is divided into two types.

Figure 4 shows three 100 forbidden dark-field images from the $x=0.12$ sample at 12 K, which was kept for 39 min, 2 sec; 39 min, 23 sec; and 39 min, 45 sec, respectively. Note that each image was obtained from the area surrounded by fine white lines in Fig. 3. The exposure time of each image was about 1.5 sec. In these images, the local *Pccn*/*LTT*-tilt regions are seen as bright contrast in the interior of the LTO domain, in addition to the regions along the twin boundary.

We will first look at the local *Pccn*/*LTT*-tilt region *A* with a size of about 50 nm. From these three images, its shape is found to change continuously with time. That is, the dynamic nature of the local region with a relatively large size

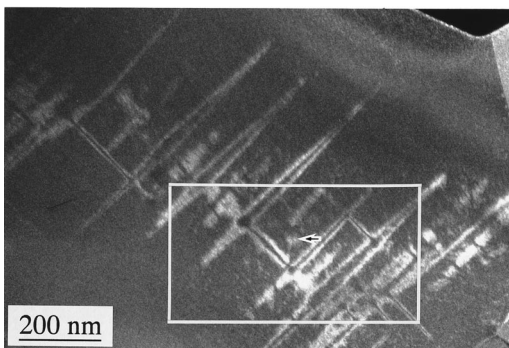


FIG. 3. 100 forbidden dark-field image of the $x=0.12$ sample at 12 K.

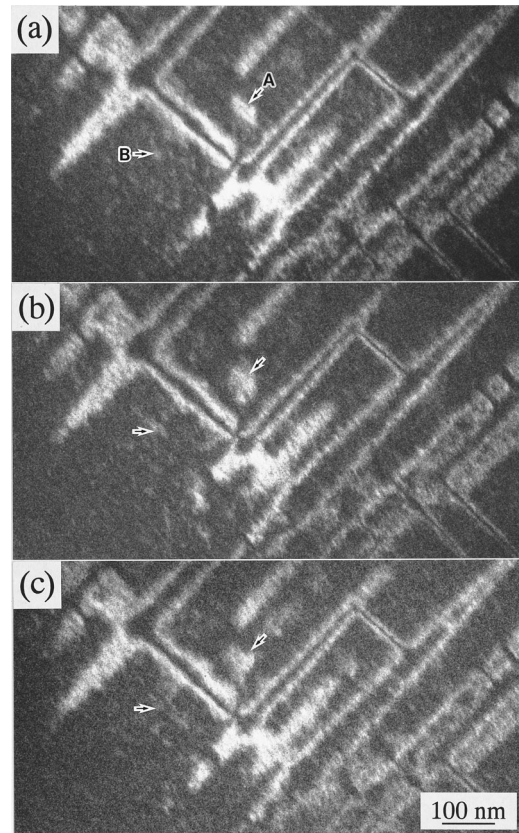


FIG. 4. A series of 100 forbidden dark-field images taken from the $x=0.12$ sample at 12 K, which were kept for (a) 39 min 2 sec, (b) 32 min 23 sec, and (c) 39 min 43 sec, respectively.

of more than about 30 nm is manifested as a continuous change in shape under a constant volume. On the other hand, the dynamic nature of the small-size region is different from that of the large one, as is observed in area *B*. It was found from the images that the local *Pccn*/*LTT* region in area *B* was about 10 nm in size and that the region was nucleated and then annihilated in a time period of about 1 min. That is, the time average of the oxygen-octahedron tilt is understood to be the LTO one. It should be mentioned again that x-ray and neutron powder diffractions made so far have not indicated the presence of the *Pccn*/*LTT* phase in $\text{La}_{2-x}\text{Sr}_x\text{CuO}_4$. This suggests that the *Pccn*/*LTT*-tilt region in the interior of the LTO domain never grows, nor does the very small volume fraction of the *Pccn*/*LTT* region along the twin boundary. The dynamic nature of the local *Pccn*/*LTT*-tilt region that was observed in the present work is concluded to be the equilibrium fluctuation of the local order parameter.

Let us mention the influence of the electron beam to the dynamic fluctuation observed in the present work. Possible factors to consider for the influence are beam heating, beam irradiation, and the charging of a specimen surface. Among these three factors, we first discuss a beam-heating effect. The beam heating just gives rise to an increase in a specimen temperature. If the temperature goes up above about 40 K, the *Pccn*/*LTT*-tilt region should be annihilated. That is, the change in the microstructure is irreversible. In addition, we did not change the operation condition in taking a series of

the dark-field images. It is not then necessary to take beam heating into account for the dynamic fluctuation. As for beam irradiation, a change is also irreversible. Actually, we detected a fade-out of an image contrast by irradiating for 10 h. It is obvious that beam irradiation has no effect on the dynamic behavior in the time period of about 1 min. The charging of a specimen surface is only a factor which may produce the dynamic fluctuation. As the specimen is a superconductor, a contact between the specimen and a grid is crucial for the fluctuation. Then we always confirmed a good contact in each experiment. So we believe that the charging is also irrelevant to the dynamic change. We therefore conclude that the dynamic fluctuation of the *Pccn*/*LTT*-tilt region should be a real phenomenon at lower temperatures around $x \approx 0.12$ in $\text{La}_{2-x}\text{Sr}_x\text{CuO}_4$.

IV. DISCUSSION

The present experimental results confirmed that a low-temperature structural phase transition occurs in $\text{La}_{2-x}\text{Sr}_x\text{CuO}_4$, which is basically characterized by the appearance of the *Pccn*/*LTT*-tilt region along the LTO twin boundary. The interesting features to note here are that only in the $x=0.115$ and 0.12 samples does the *Pccn*/*LTT*-tilt region also appear in the interior of the LTO domain at temperatures far below the transition temperature and exhibited two types of dynamic behavior. One was observed in the large-size region greater than 30 nm, where the shape of the region was continuously fluctuating under a constant volume. The other observed in the small-size region was that the region appeared and was then annihilated as time passed.

Figure 5 is a phase diagram of $\text{La}_{2-x}\text{Sr}_x\text{CuO}_4$, which was constructed from the present data. Both the superconducting transition temperature T_C and the temperature range estimated from a small pseudogap found by photoelectron spectroscopy are depicted.²¹ Note that T_L in the $x=0.115$ and 0.15 samples was, respectively, found to be 105 and 90 K, as was reported previously.¹³ It is seen in the diagram that the transition temperature T_L decreases with increasing Sr content. Surprisingly, T_L is located in the vicinity of the temperature range of the small pseudogap and exhibits the same concentration dependence. On the other hand, the dynamic fluctuation of the *Pccn*/*LTT*-tilt region in the interior of the LTO domain is detected only in the dotted area around $x=0.12$ below about 40 K. It should be mentioned that T_C was slightly suppressed in this concentration region and that the incommensurate magnetic structure was formed below about $T_N=45$ K at $x=0.12$, as marked by the solid circle.²⁰ That is, these physical phenomena are related to the dynamic *Pccn*/*LTT*-tilt region in the interior of the LTO domain. In the measurement of the longitudinal sound velocity for $x=0.12$, in fact, lattice instability toward the low-temperature transition was found below about 45 K.²⁰

As shown in the phase diagram of Fig. 5, the equilibrium fluctuation of the *Pccn*/*LTT*-tilt region in the interior of the LTO domain is present around $x=0.12$. The unique feature of the fluctuation is that it occurs in the low-temperature phases of the low-temperature structural transitions, not in a parent phase in the usual ferroelastic transition. One of reasons for the fluctuation at lower temperatures is a symmetry change in the low-temperature transitions. That is, the LTO

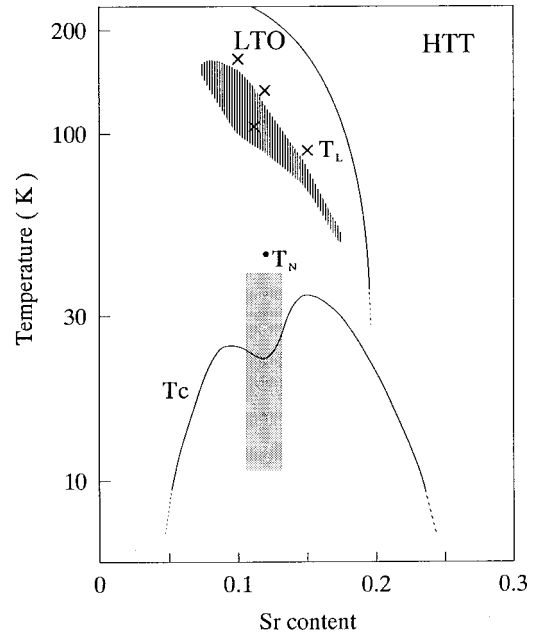


FIG. 5. Phase diagram of $\text{La}_{2-x}\text{Sr}_x\text{CuO}_4$ constructed on the basis of the present experimental data. The three-dimensional dynamic fluctuation of the *Pccn*/*LTT*-tilt region in the interior of the LTO domain is observed in the dotted area of the diagram. The hatched area is the temperature range estimated from a small pseudogap found by photoelectron spectroscopy. The transition temperature T_L of the low-temperature transition is characterized by the appearance of the *Pccn*/*LTT*-tilt region along the twin boundary. Two-dimensional local *Pccn*/*LTT* regions having dynamic nature should exist below T_L . In addition, T_N is the Néel temperature of the incommensurate magnetic structure at $x=0.12$, which was determined by Suzuki *et al.* (Ref. 20).

\rightarrow *Pccn* \rightarrow *LTT* transitions upon cooling lead to an increase in symmetry. Therefore, when a *Pccn*/*LTT* region is nucleated in a LTO domain, there is no *Pccn*/*LTT* variant to relax the strain field produced by the nucleated region. A second factor is the anisotropic long-range nature of the strain. Owing to this nature, the map of the strain order parameter is not identical to that of the local order parameter. These two factors obviously make the nucleated region unstable. So another factor to stabilize the *Pccn*/*LTT*-tilt region is definitely needed. We pay attention to the fact that the fluctuation occurs only around $x=0.12$. It is then understood that its occurrence is controlled by the hole concentration. Because there are two inequivalent sites of the oxygen ion in the CuO_2 plane of the *Pccn*/*LTT* structure, strong coupling presumably occurs between the *Pccn*/*LTT* tilt and the doped hole. In other words, a state stabilized at low temperatures around $x=1/8$, which is characterized by a three-dimensional, regular array of doped holes, should be crucial for the appearance of the *Pccn*/*LTT*-tilt region in the interior of the LTO domain. Models of the state such as a Wigner charge density wave and charge-spin stripes have been proposed.^{22–25}

Anyhow, the equilibrium fluctuation of the *Pccn*/*LTT*-tilt region is understood to result from three factors: an increase in symmetry, the anisotropic long-range nature of strain, and the stabilization of the electronic state characterized by a three-dimensional, regular array of the doped holes.

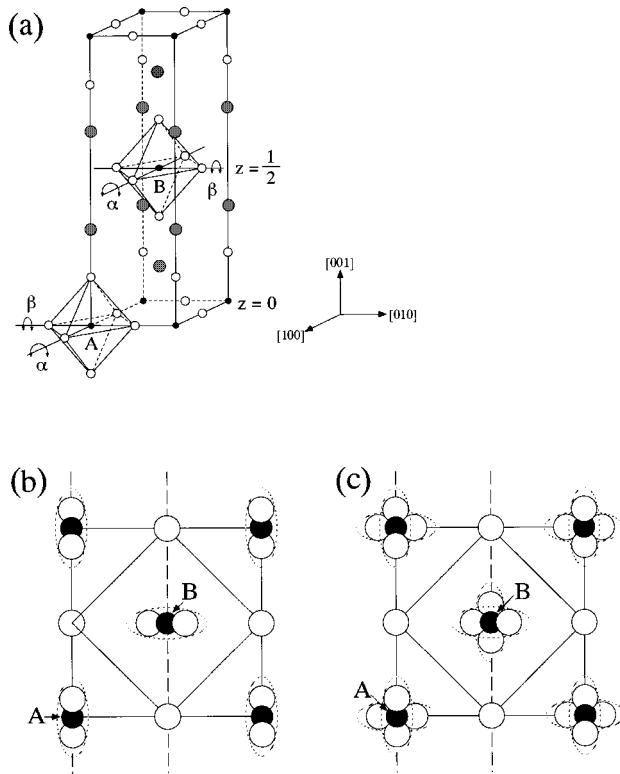


FIG. 6. (a) A unit cell of the K_2NiF_4 -type structure, (b) a [001] projection of atomic positions in the case of the perfect three-dimensional correlation of the octahedron tilt, and (c) a [001] projection in the two-dimensional case. In (a), the α and β tilts denote the CuO_6 octahedron tilts about the $[100]$ and $[010]$ directions, respectively.

The $Pccn/LTT$ -tilt region nucleated along the LTO twin boundary does not basically show dynamic behavior and is rather static, although the region is nucleated at relatively higher temperatures. It is worth noting that the octahedron in the twin boundary is tilted about the $\langle 100 \rangle$ axis, the LTT tilt, as the superposition of two $\langle 110 \rangle$ tilts in the LTO structure. That is, a nucleus of the LTT phase already exists in the twin boundary of the LTO phase. The nucleation of the $Pccn/LTT$ -tilt region along the boundary does not therefore need an activation process. In addition, the $Pccn/LTT$ -tilt region should be pinned by the twin boundary as a planar defect. That is, the pinning is thought to be a physical reason for the absence of dynamic fluctuation in the $Pccn/LTT$ -tilt region nucleated along the twin boundary.

Let us discuss the dimensionality of the local $Pccn/LTT$ -tilt region. In electron diffraction patterns, the region is characterized by the 100-type forbidden spots. From a simple calculation of the structure factor of the $Pccn/LTT$ structure, the forbidden spots basically come from the positional correlation between the apical oxygen ions of the CuO_6 octahedra in the two neighboring CuO_2 planes along the $[001]$ direction, as will be shown in the Appendix. That is, the presence of the 100-type forbidden spots reflects a three-dimensional correlation of the octahedron tilt. The three-dimensional correlation along the LTO twin boundary then occurs at T_L , although it does not occur in the interior of the LTO domain. It should be here mentioned that dynamic local LTT distortion was recently found

below 100 K in $x=0.15$ by Cu K -edge extended x-ray absorption fine structure (EXAFS) measurement.^{22,23} The local LTT distortion should be two dimensional in character. From the fact that the $Pccn/LTT$ -tilt regions are nucleated along the twin boundary around 90 K in the present $x=0.15$ sample, the appearance of the three-dimensional region along the twin boundary is understood to be an indication of that of the two-dimensional local $Pccn/LTT$ -tilt region in the interior of the LTO domain. In $La_{2-x}Sr_xCuO_4$, therefore there exist the two-dimensional local $Pccn/LTT$ -tilt regions below T_L in $0.1 \leq x \leq 0.15$, while the three-dimensional correlation of the tilt is developed only below about 40 K in the vicinity of $x=0.12$.

In $La_{2-x}Sr_xCuO_4$, T_C is slightly suppressed around $x=0.12$. As can be understood from Fig. 5, the slight suppression of T_C would be responsible for the dynamic three-dimensional fluctuation of the local order parameter, that is, the appearance of the local $Pccn/LTT$ -tilt region. Here we discuss the relation between the slight T_C suppression and the three-dimensional dynamic fluctuation found in the present work. As was already pointed out in previous papers,^{22,23,26-29} the electronic structure of the LTT-tilt structure with a large tilt angle is much different from that of the LTO-tilt one. Particularly, the LTT tilt was theoretically suggested to result in the splitting of the bands at the $1/2 0 0$ -type position $(\pi, 0, 0)$. From this suggestion, we think that the three-dimensional local $Pccn/LTT$ -tilt fluctuation would produce a pseudogap, leading to a decrease in the density of states at E_F . The slight T_C suppression can be therefore explained as being due to the existence of the three dimensional $Pccn/LTT$ -tilt region. This speculation also leads to a very important consequence. That is, if the three-dimensional $Pccn/LTT$ -tilt region is responsible for the T_C suppression, the two-dimensional local region appearing below T_L may influence the electronic structure, the formation of a similar pseudogap at $(\pi, 0, 0)$. As shown in the phase diagram in Fig. 5, the transition temperature T_L characterized by the appearance of the $Pccn/LTT$ -tilt region along the twin boundary is actually located in the vicinity of the temperature range estimated from the small pseudogap. It seems that the small pseudogap found in photoelectron spectroscopy is presumably related to the two-dimensional local $Pccn/LTT$ -tilt region.

In $La_{1.88}Sr_{0.12}CuO_4$, the static incommensurate magnetic structure was recently found near the temperature range, in which the three-dimensional fluctuation of the $Pccn/LTT$ -tilt region in the interior of the LTO domain occurs.²⁰ This indicates that the $Pccn/LTT$ tilt can stabilize the incommensurate magnetic structure. A similar magnetic structure was also reported in the LTT phase of $La_{1.48}Nd_{0.4}Sr_{0.12}CuO_4$ and interpreted to be due to the ordering of the charge-spin stripe, which is pinned by the $Pccn/LTT$ tilt.^{24,25} Based on this interpretation, the appearance of the incommensurate magnetic structure in $x=0.12$ may suggest stripe ordering in the $Pccn/LTT$ -tilt region. The ordering of the charge-spin stripe is, in fact, one of candidates of the state stabilized at lower temperature around $x=1/8$. In the present work, however, we could not detect any superlattice reflection spots exhibiting such ordering.

V. CONCLUSION

In $\text{La}_{2-x}\text{Sr}_x\text{CuO}_4$ with $0.1 \leq x \leq 0.15$, the two-dimensional local $Pccn/LTT$ -tilt region appears below T_L when the sample is cooled in the LTO phase. The three-dimensional correlation of the octahedron tilt is, on the other hand, restricted below about 40 K near $x=0.12$, where the T_C suppression and the appearance of the incommensurate magnetic structure occur. It also seems that the pseudogap found by photoelectron spectroscopy may be related to the appearance of the two-dimensional local $Pccn/LTT$ -tilt region.

ACKNOWLEDGMENT

One of us (Y.H.) would like to thank the Research Fellowships of the Japan Society for the Promotion of Science for Young Scientists for financial support.

APPENDIX

Here we explain the origin and features of the 100-type forbidden reflections, which are characterized by the $Pccn/LTT$ tilt of the CuO_6 octahedron. In this explanation, the 100-type reflections are, for simplicity, assumed to be due to the atomic displacements of the oxygen ions in the CuO_6 octahedra tilted about the $\langle 100 \rangle$ directions. That is, we treat only the displacements of the oxygen ions in the LTT tilt here. Figure 6(a) shows a unit cell of the K_2NiF_4 -type crystal structure of the $\text{La}_{2-x}\text{Sr}_x\text{CuO}_4$. In the structure, the

CuO_6 octahedra are present in two CuO_2 layers at $z=0$ and $1/2$. In each layer, there are two possible tilts, the $[100]$ and $[001]$ tilts, which are denoted by the α and β tilts, respectively. In the LTT structure where the perfect three-dimensional correlation of the tilt exists, if the α tilt takes place in the $z=0$ layer, the β tilt must occur in the $z=1/2$ layer. A $[001]$ projection of the atomic positions obtained in this case is shown in Fig. 6(b). As is seen in the projection, for instance, the projected positions around a location denoted by A is different from those around a location by B . This difference gives rise to the 100-type forbidden reflections. Because the positions deviated from the locations, A and B , in the projection originate from the atomic displacements of the apical oxygen ions in the CuO_6 octahedra, the displacements of the apical oxygen ions are responsible for the 100-type forbidden reflection. We then discuss the two-dimensional correlation case. In this case, the α and β tilts occur randomly layer by layer. A $[001]$ projection in the two-dimensional case is shown in Fig. 6(c). The projected positions around the location A is identical to those around the location B . So the two-dimensional correlation of the tilt never produces the 100-type forbidden reflection. It is therefore understood that the 100-type forbidden reflection reflects the three-dimensional correlation of the octahedron tilt about the $\langle 100 \rangle$ direction. In other words, even in the case of no 100-type reflection, the existence of the two-dimensional LTT-tilt region is still possible.

-
- ¹R. M. Fleming, B. Batlogg, R. J. Cava, and E. A. Rietman, Phys. Rev. B **35**, 7191 (1987).
 - ²A. R. Moodenbaugh, Y. Xu, M. Suenaga, T. J. Folkerts, and R. N. Shetlon, Phys. Rev. B **38**, 4596 (1988).
 - ³J. D. Axe, A. H. Moudden, D. Hohlwein, D. E. Cox, K. M. Mohanty, A. R. Moodenbaugh, and Y. Xu, Phys. Rev. Lett. **62**, 2751 (1989).
 - ⁴T. Suzuki and T. Fujita, Physica C **159**, 111 (1989).
 - ⁵M. K. Crawford, R. L. Harlow, E. M. Macaron, W. E. Farneth, J. D. Axe, H. Chou, and Q. Huang, Phys. Rev. B **44**, 7749 (1991).
 - ⁶Y. Koyama, Y. Wakabayashi, and Y. Inoue, Physica C **235-240**, 833 (1994).
 - ⁷Y. Maeno, M. Nohara, F. Nakamura, T. Suzuki, and T. Fujita, J. Supercond. **7**, 39 (1994).
 - ⁸Y. Koyama, Y. Wakabayashi, K. Ito, and Y. Inoue, Phys. Rev. B **51**, 9045 (1995).
 - ⁹Y. Inoue, Y. Horibe, and Y. Koyama, Phys. Rev. B **56**, 14 176 (1997).
 - ¹⁰Y. Horibe, Y. Inoue, and Y. Koyama, J. Supercond. **10**, 461 (1997).
 - ¹¹E. Salje, and K. Parlinski, Supercond. Sci. Technol. **4**, 93 (1991).
 - ¹²K. Parlinski, V. Heine, and E. Salje, J. Phys.: Condens. Matter **5**, 497 (1993).
 - ¹³Y. Inoue, Y. Horibe, and Y. Koyama, J. Supercond. **10**, 361 (1997).
 - ¹⁴Y. Horibe, Y. Inoue, and Y. Koyama, Physica C **282-287**, 1071 (1997).
 - ¹⁵H. Takagi, T. Ido, S. Ishibashi, M. Uota, S. Uchida, and Y. Tokura, Phys. Rev. B **40**, 2254 (1989).
 - ¹⁶I. Watanabe, K. Nishiyama, K. Nagamine, K. Kawano, and K. Kumagai, Hyperfine Interact. **86**, 603 (1994).
 - ¹⁷T. Goto, K. Chiba, M. Mori, T. Suzuki, and T. Fukase, J. Phys. Soc. Jpn. **63**, 3494 (1994).
 - ¹⁸S. Ohsugi, Y. Kitaoka, H. Yamanaka, K. Ishida, and K. Asayama, J. Phys. Soc. Jpn. **63**, 2057 (1994).
 - ¹⁹T. Goto, K. Chiba, M. Mori, T. Suzuki, and T. Fukase, J. Phys. Soc. Jpn. **66**, 2870 (1997).
 - ²⁰T. Suzuki, T. Goto, K. Chiba, T. Shinoda, T. Fukase, H. Kimura, K. Yamada, M. Ohasi, and Y. Yamaguchi, Phys. Rev. B **57**, 3229 (1998).
 - ²¹A. Ino, C. Kim, T. Mizokawa, Z.-X. Shen, A. Fujimori, M. Takaba, K. Tamasaku, H. Eisaki, and S. Uchida, J. Phys. Soc. Jpn. **68**, 1496 (1999).
 - ²²A. Bianconi, N. L. Saini, A. Lanzara, M. Missori, T. Rossetti, H. Oyanagi, H. Yamaguchi, K. Oka, and T. Ito, Phys. Rev. Lett. **76**, 3412 (1996).
 - ²³A. Lanzara, N. L. Saini, A. Bianconi, J. L. Hazemann, Y. Soldo, F. C. Chou, and D. C. Johnston, Phys. Rev. B **55**, 9120 (1997).
 - ²⁴J. M. Tranquada, B. J. Sternlieb, J. D. Axe, Y. Nakamura, and S. Uchida, Nature (London) **375**, 561 (1995).
 - ²⁵J. M. Tranquada, J. D. Axe, N. Ichikawa, Y. Nakamura, S. Uchida, and B. Nachumi, Phys. Rev. B **54**, 7489 (1996).
 - ²⁶J. Fridel, J. Phys.: Condens. Matter **1**, 7757 (1989).
 - ²⁷W. E. Pickett, R. E. Cohen, and H. Krakauer, Phys. Rev. Lett. **67**, 228 (1991).
 - ²⁸N. E. Bonesteel, T. M. Rice, and F. C. Zhang, Phys. Rev. Lett. **68**, 2684 (1992).
 - ²⁹B. Büchner, M. Breuer, A. Freimuth, and A. P. Kampf, Phys. Rev. Lett. **73**, 1841 (1994).